Table S1. EXO Sonde measurements for 2016 Yellowstone Lake PMEZ samplings

Date	Depth	Conductivity	Chlorophyll a	Phycocyanin	Temperature	pH	Dissolved Oxygen	
							mg/L	% Saturation
29-Jul-17	11.5 m	66.0 µS/cm	1.08 µg/L	0.03 µg/L	12.6 °C	8.01	8.28	100
5-Aug-17	11.0 m	67.4 µS/cm	0.81 µg/L	0.03 µg/L	13.6 °C	7.98	8.17	100

Table S2. Bacterial strains, plasmids and primers used in this study.

Plasmid, strain, primers	Relevant markers and characteristics	Reference or source
Plasmid		
pCPP30	TetR, Tra− Mob+ IncP replicon, broad host range	*Micheal Kahn, Washington St. Univ.*
pCPP30::*aat*	pCPP30 carrying the wild type *aat* for complementation of the *aat* ::Tn*5*-B22 mutant	This study
pET-28a(+)	Control expression plasmid for bioassay experiments	Novagen
pET-28a(+)::*aat*	Expression expression plasmid carrying the *aat* gene for bioassays	This study
pET-28a(+)::*aat* (K241A)	Expression expression plasmid carrying the K241A mutant *aat* gene for bioassays	This study
pSUP102	Suicide plasmid, Tn*5*- B22 delivery shuttle	*80*
pCR2.1	PCR TA cloning vector	Invitrogen
Strain		
Acidovorax sp.	Wild type *Acidovorax* strain YL-MeA-13 used for characterizations	This study
Mutant 3-29	YL-MeA-13, *aat* ::Tn*5*- B22; GentR	This study
Complemented Mutant 3-29	YL-MeA-13, *aat* ::Tn*5*- B22 mutant carrying pCPP30::*aat;* GenR, TetR	This study
Pseudomonas sp.	Lake isolate (MK896839.1)	This study
Caulobacter sp.	Lake isolate (MK896844.1)	This study
Mesorhizobium sp.	Lake isolate (MK896845.1)	This study
Dietzia sp.	Lake isolate (MK896847.1)	This study
Escherichia coli		
S17-1	$Pro^{-}Mob^{+}$; conjugation donor	Lab stock
BL21 (DE3)	F^{-} *omp* T *hsdS* $_B(r_B^{-}m_B^{-})$ *gal dcm rne* 131 (DE3) pLysS (Cam^R)	Invitrogen
Primers		
Universal *mcrA*	*mcrA* F, 5'-GGTGGTGTMGGATTCACACARTAYGCWACAGC-3' *mcrA* R, 5'-TTCATTGCRTAGTTWGGRTAGTT-3'	*74*
16S rRNA gene, near full length	27 F, 5'-AGAGTTTGATCMTGGCTCAG-3' 1492 R, 5'-TACGGYTACCTTGTTACGACTT-3'	*73*
16S rRNA gene Illumina sequencing	515F, 5'-GTGBCAGCMGCCGCGGTAA-3' 806R, 5'-GGACTACHVGGGTWTCTAAT-3'	*73*

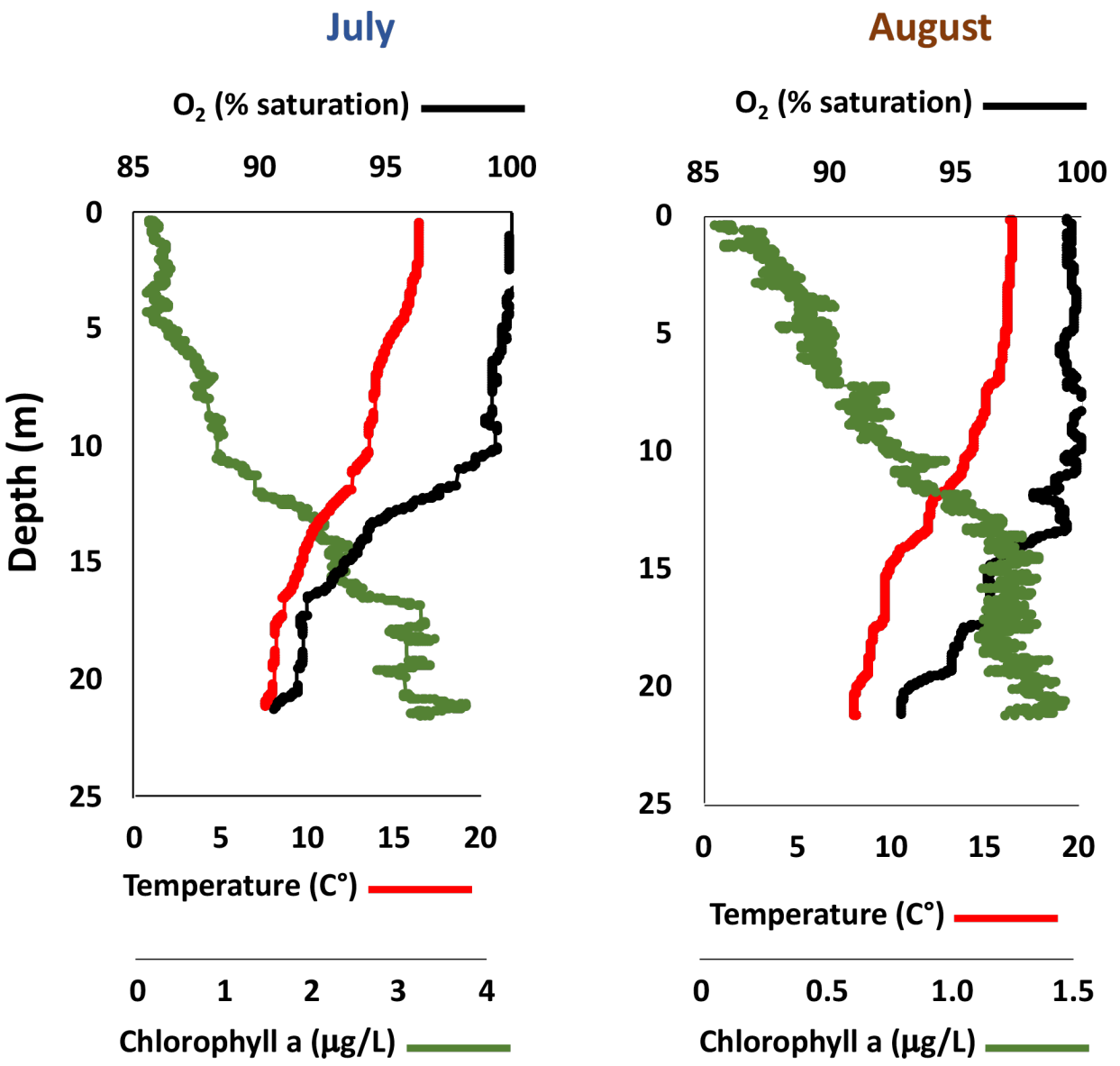

Fig. S1. EXO Sonde characterization of water column properties in 2016 samplings. Note O_2 saturation (or nearly so) at both PMEZ depths (July, 11 m; August, 11.5 m).

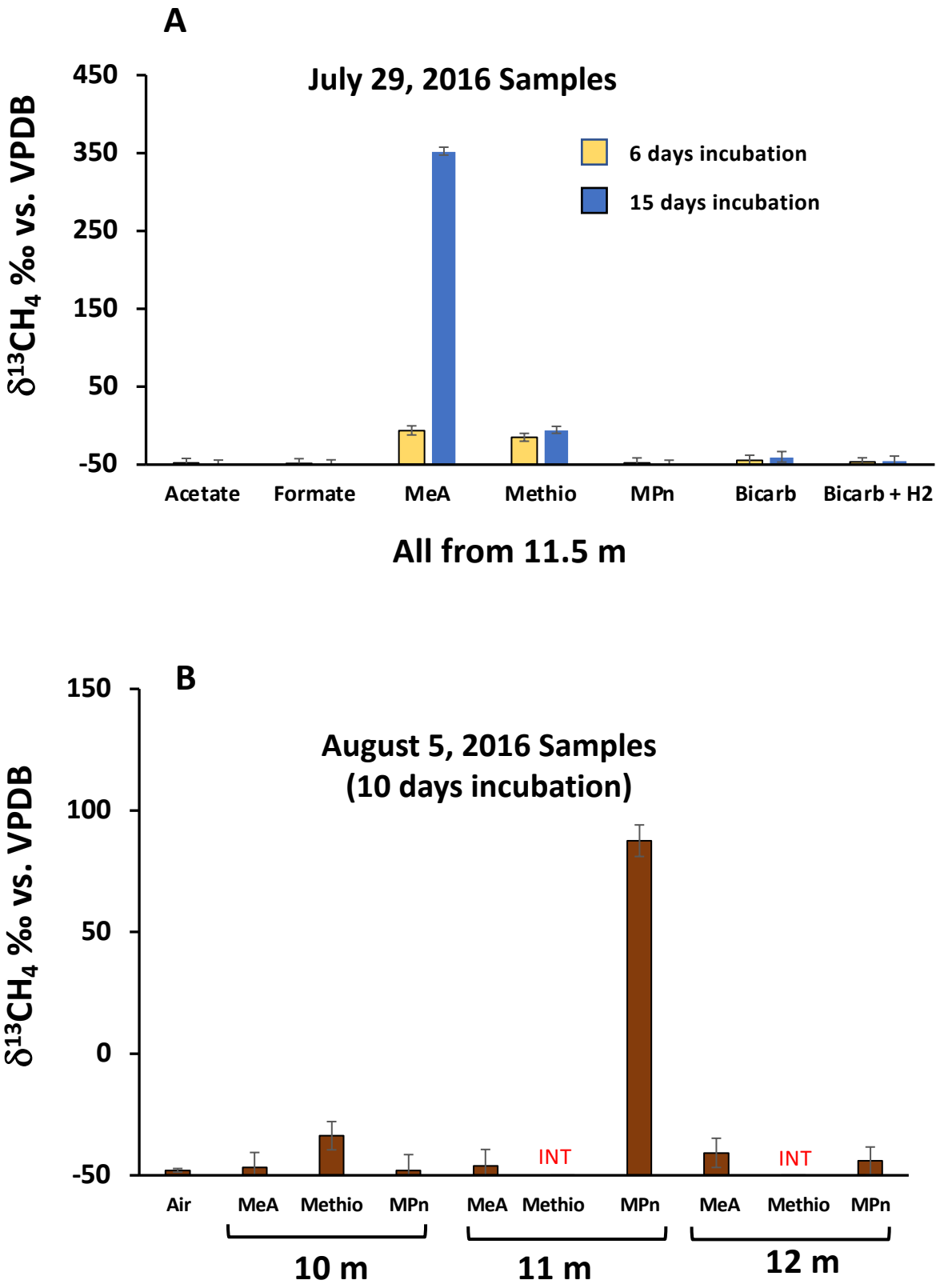

Fig. S2. $^{13}CH_4$ derived from lake water incubated with ^{13}C-labaled methylated substrates that are potentially used by methanogens for methane synthesis. Substrates used were acetate, formate, methylamine (MeA), methionine (Methio), methylphosphonate (MPn), bicarbonate (Bicarb) or bicarbonate plus hydrogen (Bicarb + H_2). Data are mean ± range of n=2 distinct water samples, INT, refers to interference from an unknown (sulfur-containing) gas.

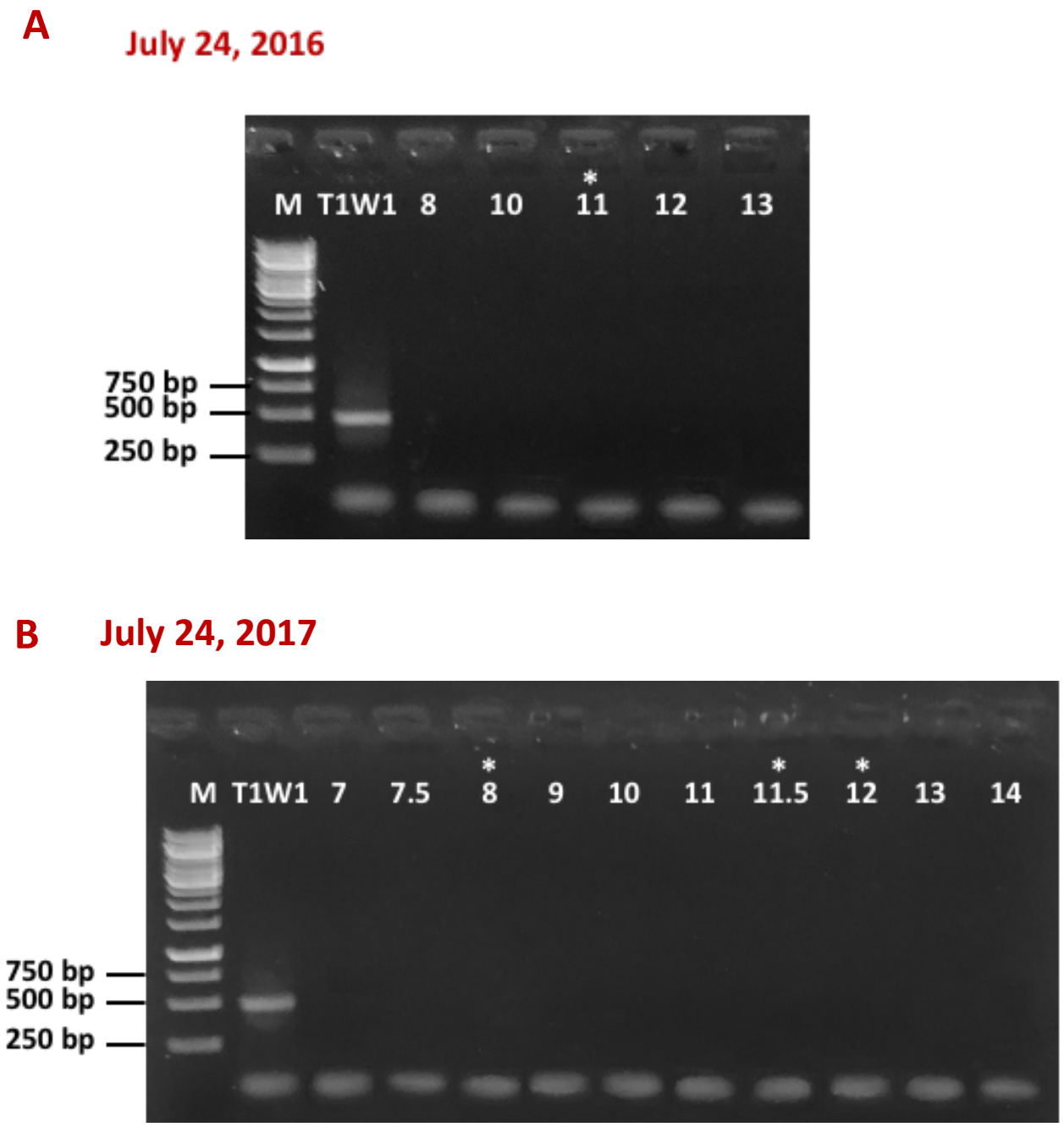

Fig. S3. PCR-based probing of Yellowstone Lake DNA for the *mcrA* gene as a proxy for presence or absence of methanogens. Universal *mcrA* primers were as described by Luton et al. (75). M, molecular weight markers, T1W1, positive control DNA from riparian environment (26) and as previously used (12). "*" denotes PMEZ depths.

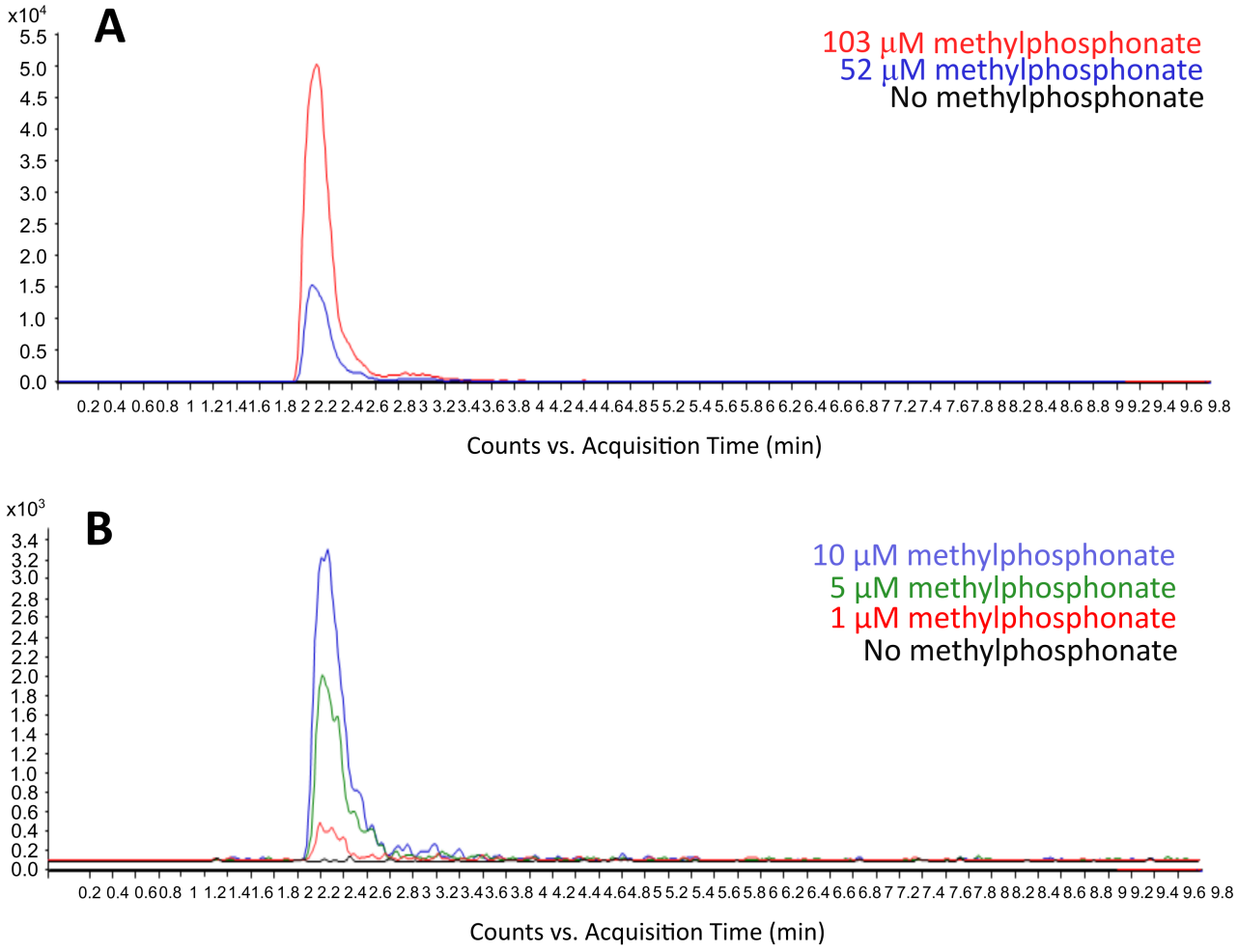

Fig. S4. LCMS analysis of methylphosphonate in Yellowstone Lake water. Lake samples failed to show any detectable signal. The black trace shows lake water without addition of exogenous MPn. Lake water was spiked with MPn at concentrations ranging from 1-103 µM. Level of detection was 1 µM. Extracted ion chromatograms (97.004 m/z) show high MPn (Panel A) and low MPn (panel B) spike concentrations from the standard addition experiment.

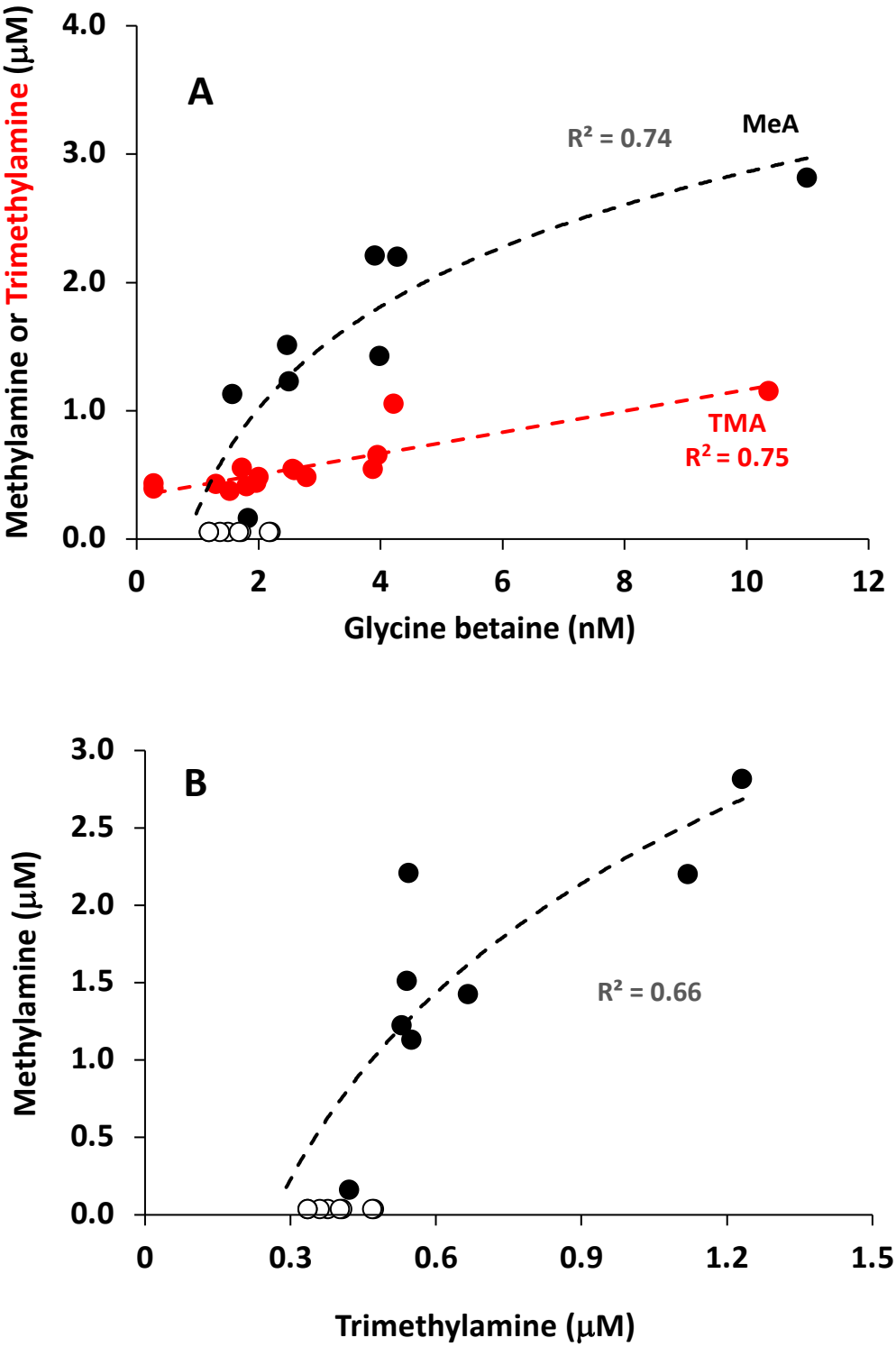

Fig. S5. Best fit regression analysis examining metabolite concentration relationships within the water column. **(A)** Correlations between glycine betaine or trimethylamine (TMA) and methylamine (MeA). **(B)** Semi Log_{10} relationship between TMA and MeA. Open symbols indicate methylamine or trimethylamine concentrations which were below detection.

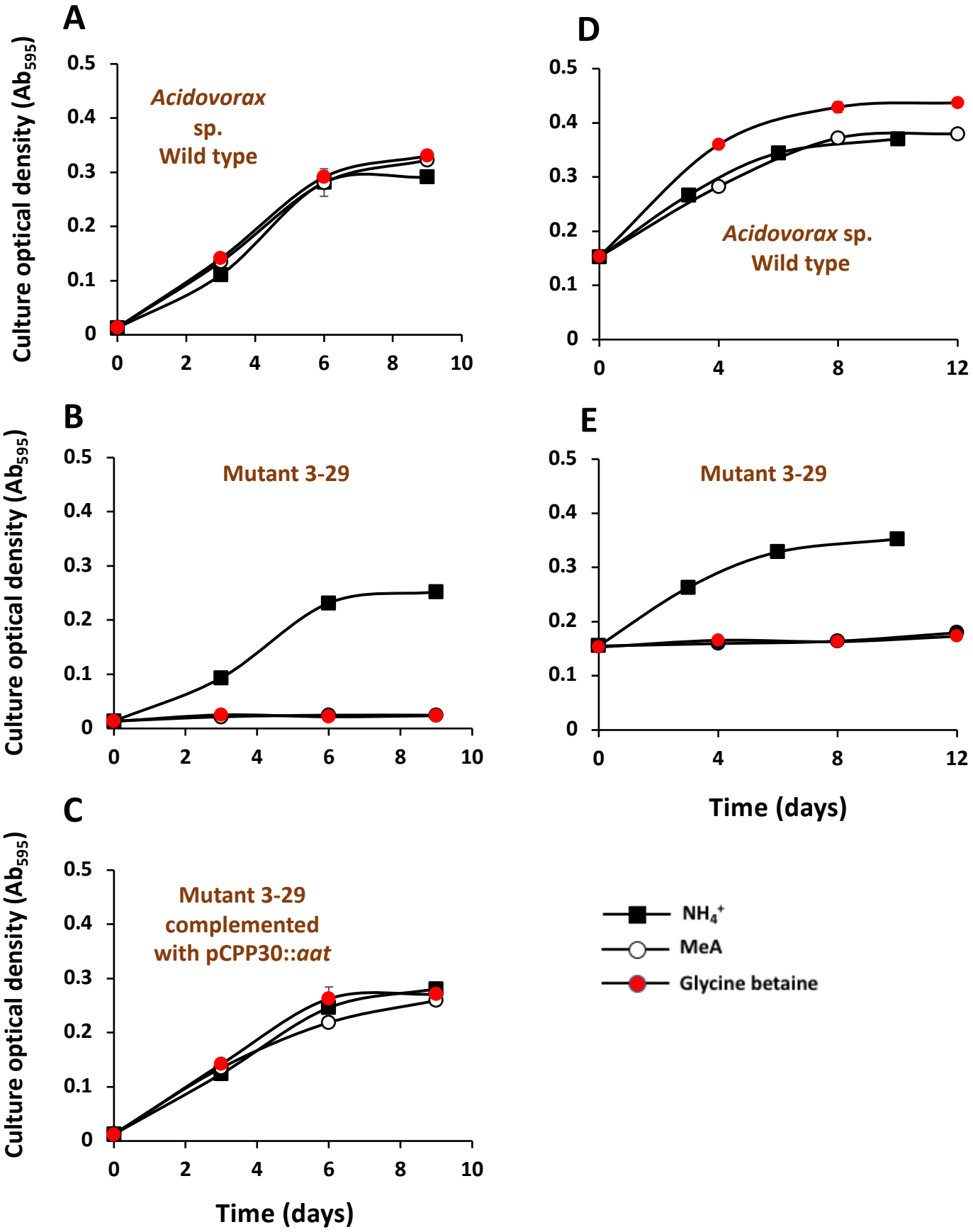

Fig. S6. Growth characteristics of the wild type, mutant, and complemented mutant strains grown with NH_4^+, methylamine (MeA), or glycine betaine (GB) as a sole N source. Cultures in panels A, B, and C were initiated at O.D.s 0.011-0.014 to illustrate how methane production from MeA is linked to growth (compare to Fig. 3). Cultures depicted in panels D and E were initiated at ~10-fold higher O.D. (Ab_{595} = 0.15) that was roughly equivalent to mid log phase of cultures in A,B, C, to illustrate that lack of methane production in the mutant is not due to lack of biomass. All data points and error bars (where visible) are the mean ± range from duplicate cultures.

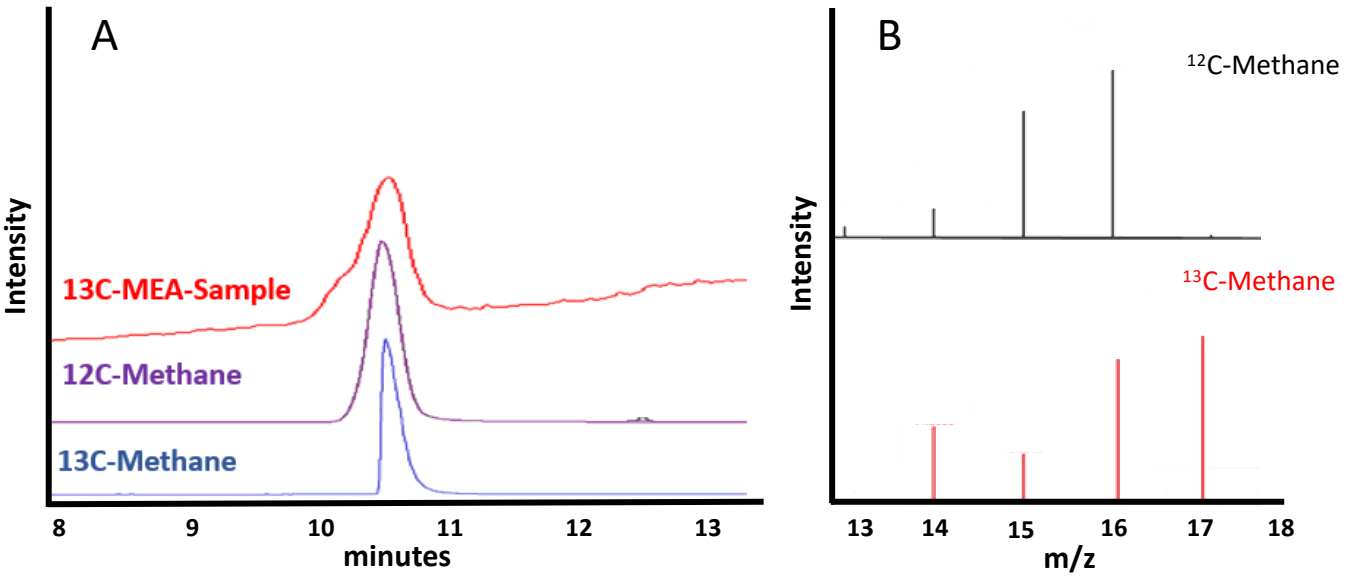

Figure S7. Transfer of ^{13}C from MeA to CH_4. **(A)** Overlaid extracted ion chromatograms corresponding to $^{13}CH_4$ (m/z=17) in headspace gas sample (^{13}C-MEA) from *Acidovorax* sp. cultured with ^{13}C-MeA as a sole N source, a $^{12}CH_4$ standard (m/z=16), and $^{13}CH_4$. **(B)** Mass spectra of CH_4 peaks from *Acidovorax sp*. cultures supplied with $^{12}CH_4$ or $^{13}CH_4$.

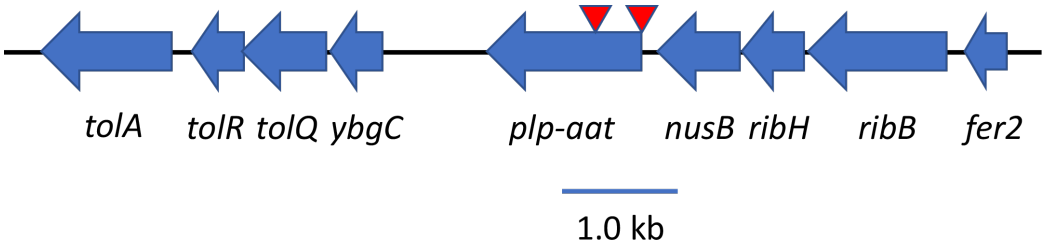

Fig. S8. Physical description of the *plp-aat* gene, adjacent DNA, and Tn5B22 insertion sites. Positions of the Tn*5*B22 insertion sites are indicated by inverted red arrowheads. Gene annotation as described in the *Acidovorax* sp. YL-MeA13-2016 genome (DOE IMG Gold Project ID Gp0440505): *tolA*, colicin import membrane protein; *tolR*, biopolymer transport TolR; *tolQ,*, biopolymer transport TolQ; *ybgC*, Tol-Pal system-associated acyl-CoA thiotolerase; plp-aat, pyrodixal phosphate-dependent aspartate aminotransferase; nusB, Nutilization substance B; ribH, dimethyl-8-ribitllumazine synthase; and rib, dihydroxy-2-butanone-4-phosphate synthase; *fer2*, ferredoxin-like. Note that the gene we describe as *plp-aat* is annotated by the JGI as "aspartate/methionine/tyrosine aminotransferase. Genbank annotation and manual BLAST searches conclude that aspartate aminotransferase is a better annotation.

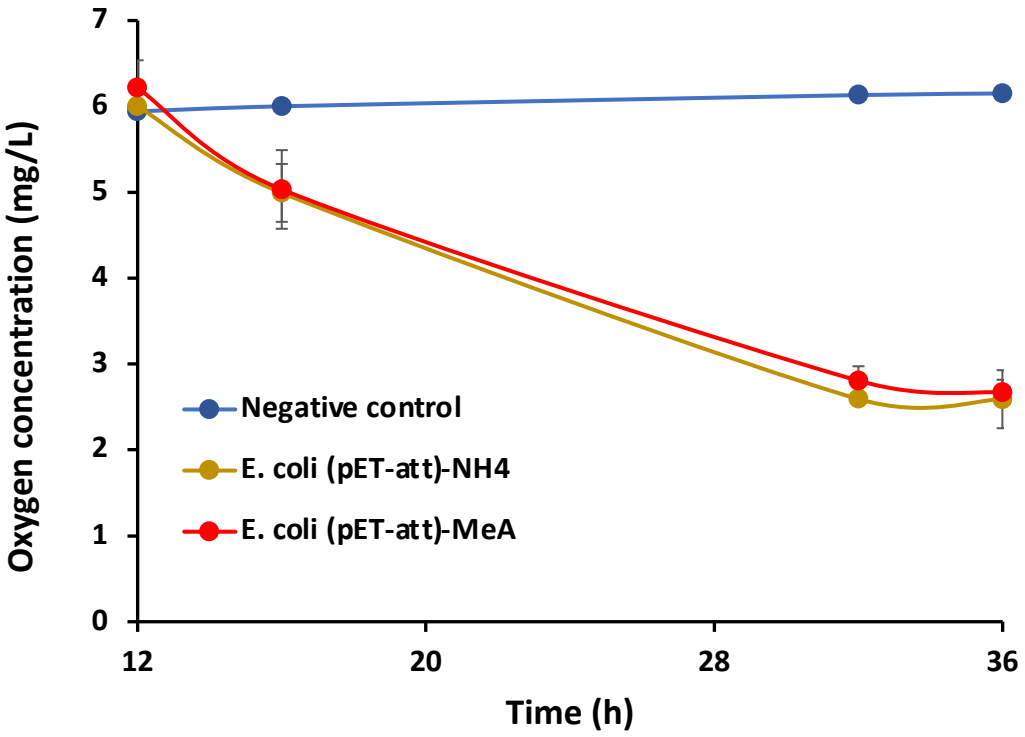

Fig. S9. Oxygen profile of CH_4 synthesizing *E.coli* BL21 carrying the recombinant *aat* cloned from *Acidovorax*. Negative controls were not inoculated. Data and error bars (where visible) represent the mean ± SD of three replicate cultures.

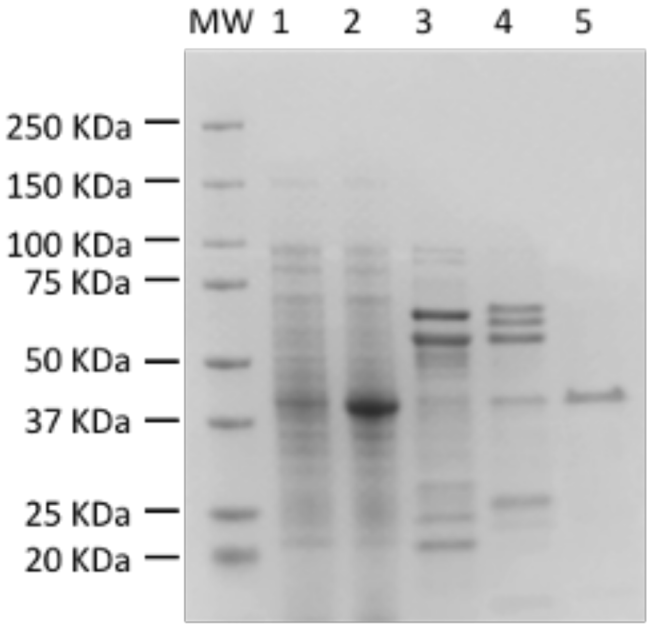

Fig. S10. SDS-PAGE profile of purified Aat protein. The soluble protein fractions from *E. coli* BL21 were purified as a His-tagged proteins using a nickel column. Lane 1, non-induced protein. Lane 2, induced total soluble protein. Lane 3, proteins eluted with 40 mM imidazole. Lane 4, protein eluted with 100 mM imidazole. Lane 5, Ni purified fraction containing Aat.

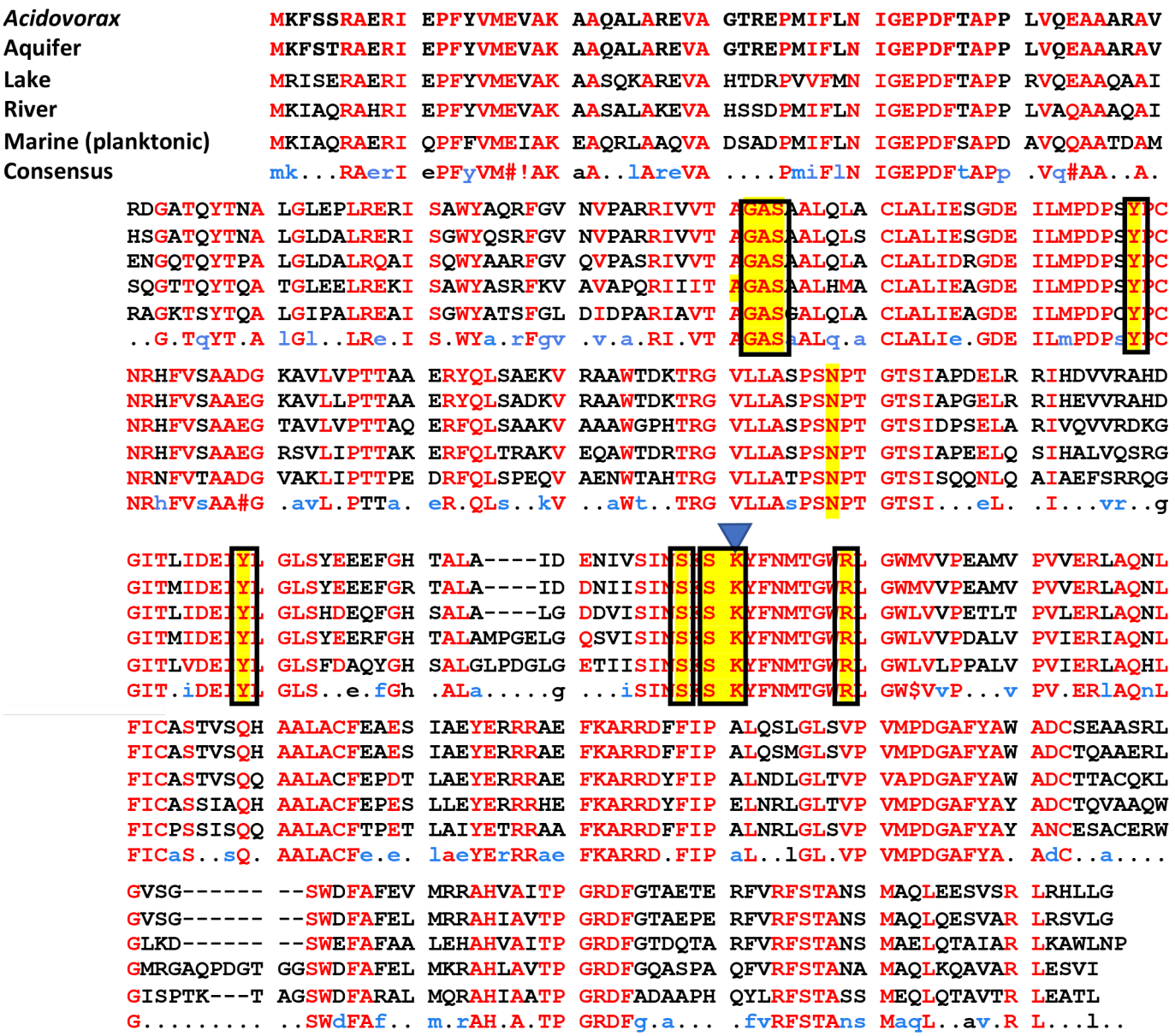

Figure S11. PLP-Aat homologs occur in other aquatic environments. Examples of PLP-Aat amino acid sequences sharing significant homology with the *Acidovorax* PLP-Aat. Aquifer, metagenome accession classified as a *Burkholderiales* protein (OGA61428); Lake, *Limnohabitans* isolate (WP_108287182); River, a *Polaromonas* sp. river isolate (TAG32972); and Marine metagenome, hypothetical protein GOS_617153 from The Sorcerer II Global Ocean Sampling Expedition (EDH37539). Inverted blue arrowhead denotes the catalytic lysine (K) that is invariant among PPL-Aat enzymes of plants, bacteria, archaea, and animals. Yellow highlighted residues designate PLP binding sites or the active site (K).